Nonequilibrium dynamics in the complex Ginzburg-Landau equation

Sanjay Puri,[1] Subir K. Das,[1] and M. C. Cross[2]
[1]*School of Physical Sciences, Jawaharlal Nehru University, New Delhi–110067, India*
[2]*Department of Physics, California Institute of Technology, Pasadena, California 91125*
(Received 18 June 2001; published 30 October 2001)

Results from a comprehensive analytical and numerical study of nonequilibrium dynamics in the two-dimensional complex Ginzburg-Landau equation have been presented. In particular, spiral defects have been used to characterize the domain growth law and the evolution morphology. An asymptotic analysis of the single-spiral correlation function shows a sequence of singularities—analogous to those seen for time-dependent Ginzburg-Landau models with $O(n)$ symmetry, where n is even.

DOI: 10.1103/PhysRevE.64.056140 PACS number(s): 64.60.Cn, 05.70.Ln, 74.20.De

Much recent interest has focused on pattern formation in the complex Ginzburg-Landau (CGL) equation

$$\frac{\partial \psi(\vec{r},t)}{\partial t} = \psi(\vec{r},t) + (1+i\alpha)\nabla^2\psi(\vec{r},t) - (1+i\beta)|\psi(\vec{r},t)|^2\psi(\vec{r},t), \quad (1)$$

where $\psi(\vec{r},t)$ is a complex order-parameter field that depends on space $(\vec{r})$ and time (t). In Eq. (1), α and β are real parameters. The CGL equation arises in a range of diverse contexts, as reviewed by Cross and Hohenberg [1]. This universality arises from the fact that the CGL equation provides a generic description of oscillations in a spatially-extended system near a Hopf bifurcation [2].

The CGL equation exhibits rich dynamical behavior with variation of the parameters α and β, and the ''phase diagram'' has been investigated (mostly numerically) in various studies [3]. In a large range of parameter space, the emergence and interaction of spiral defect structures characterizes the morphology. In this paper, we study the nonequilibrium dynamics of the CGL equation resulting from a small-amplitude random initial condition. In general, this nonequilibrium evolution is referred to as ''phase ordering dynamics'' or ''domain growth,'' and constitutes a well-studied example of far-from-equilibrium statistical physics [4,5]. Our analytical understanding of phase ordering systems has depended critically upon modeling the dynamics of defects in these systems (e.g., interfaces, vortices, monopoles, etc.) [5–8]. In this communication, we use spiral defect structures to characterize the evolution morphology in the CGL equation. Many important features emerge in our study, which should be of great relevance for both experiments and subsequent numerical simulations.

For simplicity, we will focus on the CGL equation with $\alpha=0$ and dimensionality $d=2$. However, the results presented here are also relevant for the cases with $\alpha\neq 0$ and $d>2$, as the underlying paradigm does not change, i.e., spirals continue to determine the morphology in large regions of parameter space. Following the work of Hagan [9], Aranson *et al.* [10], and Chate and Manneville [3], let us briefly discuss the phase diagram of the $d=2$ CGL equation with $\alpha=0$. The limiting case $\beta=0$ corresponds to the dynamical XY model, which is well understood. The appropriate (point) defects are vortices, and domain growth is driven by the attraction and annihilation of vortex-antivortex pairs. The relevant growth law for the characteristic length scale is $L(t)\sim(t/\ln t)^{1/2}$ [11,5]; and the analytic form of the time-dependent correlation function (which characterizes the evolving morphology) has been obtained by Bray and Puri, and (independently) Toyoki [7]. Without loss of generality, we focus on the case with $\beta\geqslant 0$. For $0\leqslant\beta\leqslant\beta_1$ ($\beta_1\simeq 1.397$ [9]), spirals (which are asymptotically plane waves) are linearly stable to fluctuations. For $\beta_1<\beta\leqslant\beta_2$ ($\beta_2\simeq 1.82$ [10,3]), spirals are linearly unstable to fluctuations, but the growing fluctuations are advected away, i.e., the spiral structure is globally stable. Finally, for $\beta_2<\beta$, the spirals are globally unstable and cannot exist for extended times [10]. Our results are relevant for the parameter regime with $\beta\leqslant\beta_2$, where spiral defects are an important feature of the morphology.

Figure 1 shows the typical evolution from a small-amplitude random initial condition for the case with $\beta=0.75$. Our numerical simulations were performed by implementing an isotropic Euler-discretization of Eq. (1) on N^2-lattices ($N=256$ for Fig. 1), with periodic boundary conditions in both directions. The discretization mesh sizes were $\Delta t=0.01$ and $\Delta x=1.0$. In Fig. 1, we plot constant-phase regions and the relevant color coding is provided in the figure caption. The evolving morphology is characterized by spirals and antispirals, and there is a typical length scale L, e.g., inter spiral spacing or the square root of inverse defect density, which is the definition we will use subsequently.

Figure 2(a) plots $\ln[L(t)]$ vs $\ln t$ for five representative values of β. The length-scale data was obtained from five independent runs on N^2 lattices with $N=1024$. After an initial transient period, the length scale $L(t)$ should saturate to an equilibrium value (L_s) because of an effective spiral-antispiral repulsive potential [1]. However, we stress that the local order parameter continues to be time dependent—only the morphology of the system undergoes statistical ''freezing.'' This should be contrasted with the $\beta=0$ case, where vortices continue to anneal (at zero temperature) as $t\to\infty$. As a matter of fact, the data for $\beta=0.25,0.5$ in Fig. 2(a) does not exhibit this morphological freezing on the time scales of our simulation, though signs of the crossover are evident for $\beta=0.5$.

To understand this crossover behavior, we recall the analytical solution for an m-armed spiral due to Hagan [9]

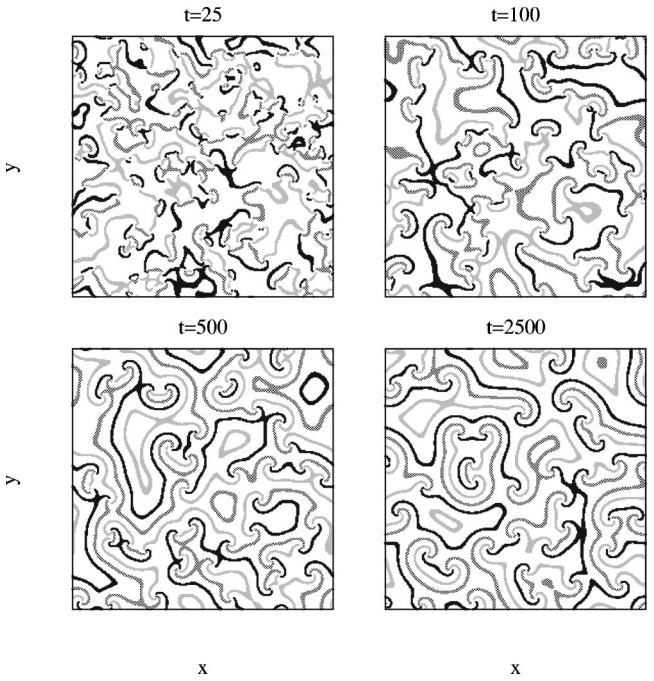

FIG. 1. Evolution of the CGL equation from a small-amplitude random initial condition. The evolution pictures were obtained from an Euler-discretized version of Eq. (1) with $\alpha=0$, $\beta=0.75$, implemented on an N^2 lattice ($N=256$). The discretization mesh sizes were $\Delta t=0.01$, $\Delta x=1.0$; and periodic boundary conditions were imposed in both directions. The snapshots show regions of constant phase $\theta_\psi=\tan^{-1}(\mathrm{Im}\,\psi/\mathrm{Re}\,\psi)$, measured in radians, with the following color coding: $\theta_\psi\in[1.85,2.15]$ (black); $[3.85,4.15]$ (dark gray); $[5.85,6.15]$ (gray). The snapshots are labeled by the appropriate evolution times.

$$\psi(\vec{r},t)=\rho(r)\exp[-i\omega t+im\theta-i\phi(r)], \tag{2}$$

where $\vec{r}\equiv(r,\theta)$; and $\omega=\beta(1-q^2)$, where q is a constant that is determined by β [9]. The limiting forms of the functions $\rho(r)$ and $\phi(r)$ are

$$\rho(r)\to\sqrt{1-q^2},\qquad \phi'(r)\to q,\quad \text{as}\quad r\to\infty,$$
$$\rho(r)\to ar^m,\qquad \phi'(r)\to r,\quad \text{as}\quad r\to 0, \tag{3}$$

where a is a constant that is determined by finiteness conditions. We will focus on the case with $m=\pm 1$, as only one-armed spirals are stable in the evolution [9]. Furthermore, we are only interested in distances $r\gg\xi$, where ξ is the defect core size. Our numerical results show that the order-parameter amplitude saturates to its maximum value on a length scale $\xi\sim O(1)$ dimensionless unit. In Table I, we present typical values of ξ for the different values of β considered here. We define ξ as the radial distance from the spiral center where the order-parameter amplitude reaches half its maximum value. On the other hand, the maximum defect length scale for (say) $\beta=1.25$ in Fig 2(a) is $L_s\simeq 13.0$. Thus, we consider the spiral form in Eq. (2) with $\rho(r)=\sqrt{1-q^2}$ and $\phi(r)=qr$ (appropriate for $r\to\infty$).

We expect that spirals behave similarly to vortices for $L<L_c$, where $qL_c\sim O(1)$. This is because the distinction between a spiral and a vortex is only apparent on length scales $qr>1$. Thus, the early evolution should be analogous to that for the XY model, both in terms of the domain growth law and correlation function. In Fig. 2(a), the solid line has a

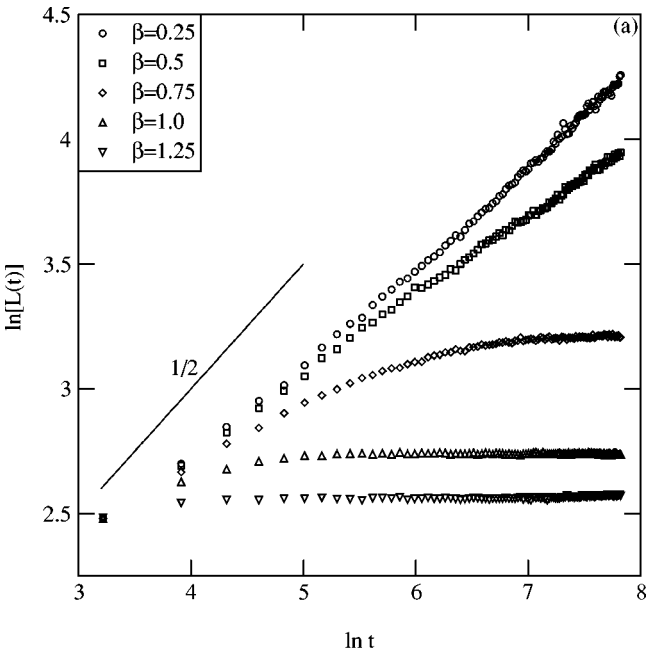

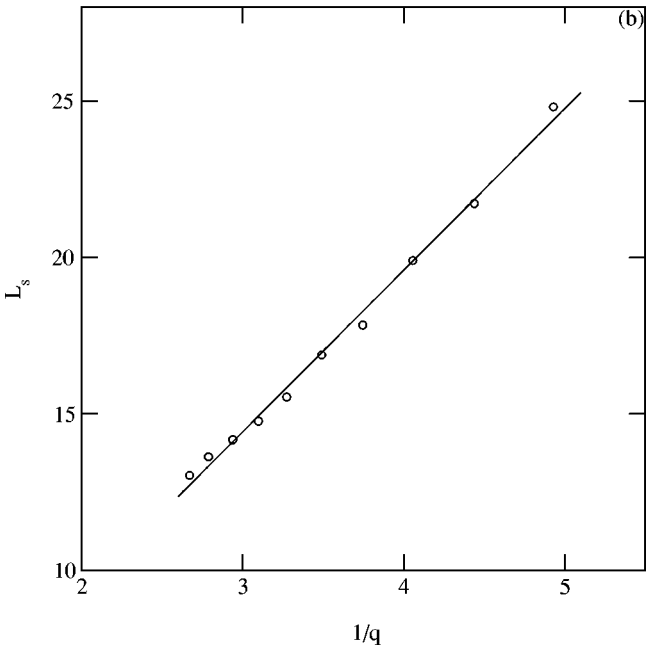

FIG. 2. (a) Plot of $\ln[L(t)]$ vs $\ln t$ for $\alpha=0$ and $\beta=0.25,0.5,0.75,1.0,1.25$—denoted by the specified symbols. The characteristic length scale $L(t)$ is obtained from the square root of the inverse defect density—measured directly from snapshots as shown in Fig. 1. The numerical data shown here were obtained as an average over five independent runs for N^2 lattices (with $N=1024$). The solid line has a slope of 1/2. (b) Plot of saturation length L_s vs q^{-1} for β values ranging from 0.75 to 1.20. The corresponding values of q (as a function of β) are obtained from Hagan's solution, cf. Fig. 5 of Ref. [9]. The solid line denotes the best linear fit to the numerical data.

TABLE I. Spiral core size (ξ) for different values of β. We define ξ as the radial distance from the spiral center where the order-parameter amplitude reaches half its maximum value.

β	0.0	0.25	0.50	0.75	1.0	1.25
ξ	0.997	1.002	1.014	1.025	1.031	1.032

slope of 1/2 and the initial growth (at least for $\beta \leqslant 0.75$) appears to be comparable with the behavior for the XY model, i.e., $L(t) \sim (t/\ln t)^{1/2}$ for $d=2$. Over extended time intervals, this growth law is similar to power-law growth with an ''effective exponent'' less than 1/2 [12]. From scaling arguments, we also expect the saturation length L_s to scale with L_c. Figure 2(b) plots L_s vs q^{-1} for a range of β values, and demonstrates that our numerical data is consistent with $L_s \sim q^{-1}$. We can also obtain the scaling law for the crossover time and the corresponding numerical results (not shown here) are in agreement with it.

Next, we consider the correlation function for the evolution morphology shown in Fig. 1. It is obviously relevant to first consider the correlation function for a single spiral of length L, as the snapshots in Fig. 1 can be thought of as consisting of disjoint spirals of size L. (Of course, this ignores modulations of the order parameter at spiral-spiral boundaries but we will discuss those later). We have approximated the one-armed single-spiral solution as $\psi(\vec{r},t) \simeq \sqrt{1-q^2}\exp[-i\omega t + i(\theta - qr)]$. The correlation function is obtained by considering the correlation between points $\vec{r}_1$ and $\vec{r}_2$ $(=\vec{r}_1+\vec{r}_{12})$ and integrating over $\vec{r}_1$ as follows:

$$C(r_{12}) = \frac{1}{V}\int d\vec{r}_1 \,\mathrm{Re}\{\psi(\vec{r}_1,t)\psi(\vec{r}_2,t)^*\}h(L-r_2)$$
$$= \frac{(1-q^2)}{V}\,\mathrm{Re}\int d\vec{r}_1 \exp[i(\theta_1-\theta_2-qr_1 + q|\vec{r}_1+\vec{r}_{12}|)]h(L-|\vec{r}_1+\vec{r}_{12}|), \quad (4)$$

where V is the spiral volume; and we have introduced the step function $h(x)=1$ (0) if $x \geqslant 0$ $(x<0)$. The step function ensures that we do not include points which lie outside the defect of size L.

It is convenient to introduce variables $\theta_1 - \theta_{12} = \theta$; $x = r_1/L$; $r = r_{12}/L$, to obtain

$$C(r_{12}) = \frac{(1-q^2)}{\pi}\,\mathrm{Re}\int_0^1 dx x \int_0^{2\pi} d\theta \frac{x + re^{i\theta}}{(x^2+r^2+2xr\cos\theta)^{1/2}} \times \exp[-iqL\{x-(x^2+r^2+2xr\cos\theta)^{1/2}\}] \times h[1-(x^2+r^2+2xr\cos\theta)^{1/2}], \quad (5)$$

where we have used $V=\pi L^2$ in $d=2$. Thus, the scaling form of the single-spiral correlation function is $C(r_{12})/C(0) \equiv g(r_{12}/L, q^2L^2)$. In general, there is no scaling with the spiral size because of the additional factor qL. We recover scaling only in the limit $q=0$ $(\beta=0)$, which corresponds to the case of a vortex. Essentially, spirals of different sizes are not morphologically equivalent because there is more rotation in the phase as one goes out further from the core.

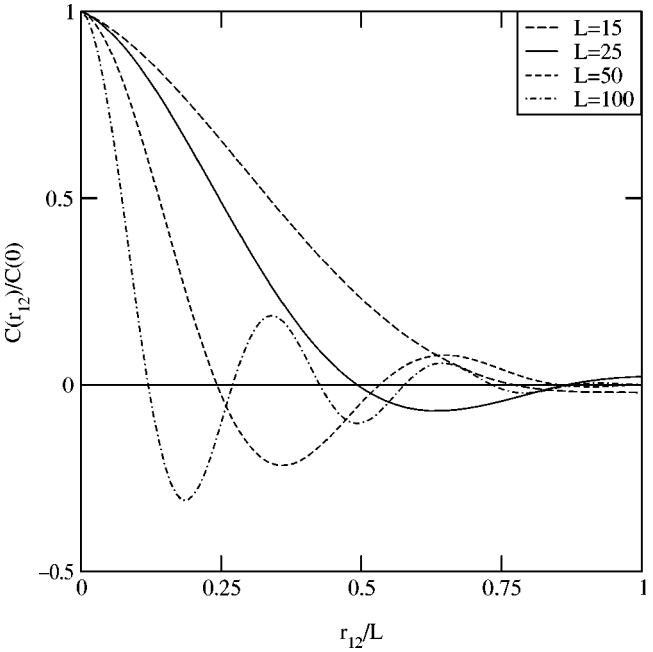

FIG. 3. Correlation function for the one-armed spiral solution when $\beta=0.75$ ($q \simeq 0.203$). We plot $C(r_{12})/C(0)$ vs r_{12}/L for different spiral sizes, $L=15,25,50,100$—denoted by the specified line types. These results are obtained from a direct numerical integration of Eq. (5).

Figure 3 plots $C(r_{12})/C(0)$ vs r_{12}/L for the case with $\beta=0.75$ ($q \simeq 0.203$). These results are obtained by a direct numerical integration of Eq. (5). We consider four different values of L. The functional form in Fig. 3 exhibits near-monotonic behavior for small values of L (i.e., in the vortex or XY limit); and pronounced oscillatory behavior for larger values of L, as is expected from the integral expression. Notice that $r_{12}/L \leqslant 2$—larger values of r_{12} correspond to the point $\vec{r}_2$ lying outside the defect.

The asymptotic behavior of the correlation function in the limit $r = r_{12}/L \to 0$ (though $r_{12}/\xi \gg 1$) is of considerable importance as it determines the tail of the momentum-space structure factor [5]. In particular, we are interested in the singular part of the correlation function as $r \to 0$. In this limit, we can discard the step function in Eq. (5) as it only provides corrections at the edge of the defect. The asymptotic analysis of the integral in Eq. (5) involves considerable algebra, which we will report in detail elsewhere. Here, we confine ourselves to quoting the final result for the singular part of $C(r_{12})$,

$$C_{\mathrm{sing}}(r_{12}) = \frac{1}{2}\sum_{p=0}^{\infty}\sum_{m=0}^{\infty}(-1)^{p+m}\frac{(qL)^{2(p+m)}}{(2p)!(2m)!} \times \frac{\Gamma(\frac{1}{2}+m)^2}{\Gamma(\frac{1}{2}-p)^2(m+p+1)!^2} \times (2m+1)(2p+1)r^{2(m+p+1)}\ln r. \quad (6)$$

Equation (6) is one of the central results of this paper and we would like to briefly discuss its implications. The leading-order singularity is the same as that for the XY model ($\beta=q=0$), $C_{\rm sing}(r_{12})=\frac{1}{2}r^2\ln r$ [13], as expected. However, there is also a sequence of subdominant singularities proportional to $(qL)^2r^4\ln r$, $(qL)^4r^6\ln r$, etc., and these become increasingly important as the length scale L increases. These subdominant terms in $C_{\rm sing}(r_{12})$ are reminiscent of the leading-order singularities in models with $O(n)$ symmetry, where n is even [5,13]. Of course, in the context of $O(n)$ models, these singularities only arise for $n\leqslant d$ as there are no topological defects unless this condition is satisfied. In the present context, all these terms are already present for $d=2$. The implication for the structure-factor tail is a sequence of power-law decays with $S(k)\sim(qL)^{2(m-1)}L^d/(kL)^{d+2m}$, where $m=1,2$, etc. Thus, though the true asymptotic behavior in $d=2$ is still the generalized Porod tail, $S(k)\sim L^2(kL)^{-4}$, it may be difficult to disentangle this from other power-law decays.

Finally, Fig. 4 compares our numerical data for the correlation function with the functional form of the single-spiral correlation function. Recall that the correlation function does not scale with the characteristic length because of the spiral nature of the defects. In Figs. 4(a)–(c), we have plotted numerical data for $C(r_{12},t)/C(0,t)$ vs r_{12} at $t=500$, and $\beta=0.75,1.0,1.25$. For the comparison with Eq. (5), the length scale L is taken to be an adjustable parameter. In each case, the best-fit value of L matches the length scale obtained from the inverse defect density [see Fig. 2(a)] within 10%. As is seen from Fig. 4, the single-spiral correlation function is in good agreement with the numerical data for the multispiral morphology up to (approximately) the first minimum. As a matter of fact, the agreement is excellent (perhaps fortuitously) for $\beta=1.25$, shown in Fig. 4(c). We should remark that the correlation function data shown in Figs. 4(b) and (c) (corresponding to $\beta=1.0,1.25$) does not change at later times, because the defect length scales have already frozen by $t=500$ for these β values [see Fig. 2(a)].

In the context of phase ordering dynamics, the Gaussian auxiliary field (GAF) ansatz [5–8] has proven particularly useful for the characterization of multidefect morphologies. We have critically examined the utility of the GAF ansatz in the present context [14] and find that it is only reasonable at early times—where, in any case, the ordering process is analogous to that for the XY model. We are presently studying methods of improving the GAF ansatz for the CGL equation and will discuss this elsewhere.

More generally, the utility of the GAF ansatz arises from the summation over phases from many defects, which results in a near-Gaussian distribution for the auxiliary field. However, in the present context, the shocks between spirals effectively isolate one spiral region from the influence of other regions. As a matter of fact, the waves from other spirals decay exponentially through the shock and the phase of a point is always dominated by the nearest spiral. Therefore, we expect that the correlation function will be dominated by the single-spiral result—in accordance with our numerical results.

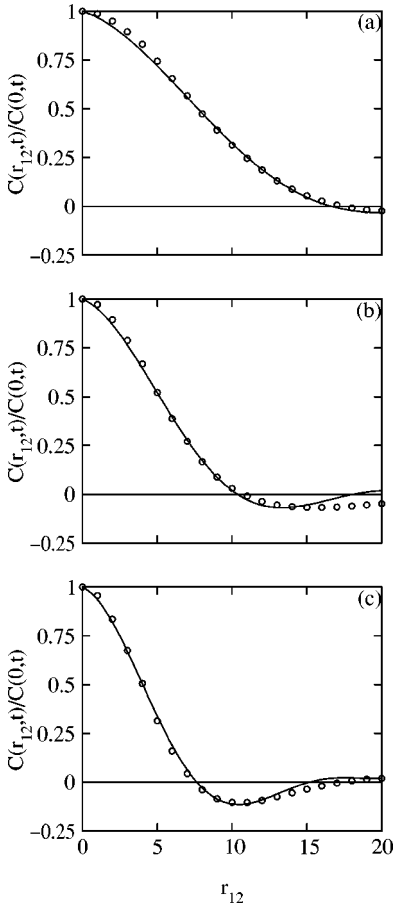

FIG. 4. Numerical data for the correlation function $C(r_{12},t)/C(0,t)$ vs r_{12} at $t=500$ for the cases $\alpha=0$ and (a) $\beta=0.75$; (b) $\beta=1.0$; (c) $\beta=1.25$. The numerical data were obtained as an average over five independent runs for N^2 lattices (with $N=1024$). The solid line refers to the numerical integration of Eq. (5) with L as an adjustable parameter. Subsequently, the r_{12} axis is scaled so that the point $C(r_{12},t)/C(0,t)=1/2$ is matched for the numerical data and the analytical expression.

To summarize, we have undertaken a detailed analytical and numerical study of nonequilibrium dynamics in the CGL equation. For early times ($L<L_c\sim q^{-1}$), the domain growth process is analogous to that for the XY model, which is well understood. At later times, distinct effects due to spirals are seen and the evolving system freezes (in a statistical sense) into a multispiral morphology. We have undertaken an asymptotic analysis of the correlation function $C(r_{12})$ for a single spiral. It exhibits a sequence of singularities as $r_{12}/L\to 0$. Furthermore, this correlation function is in good agreement with the numerical data for multispiral morphologies, over an extended range of distances.

S.P. is grateful to A.J. Bray and H. Chate for useful discussions. S.K.D. is grateful to the University Grants Commission, India, for financial support. M.C.C. thanks the School of Physical Sciences, JNU, for hospitality during the stay in which this work was begun.

[1] M.C. Cross and P.C. Hohenberg, Rev. Mod. Phys. **65**, 851 (1993).

[2] For example, see Y. Kuramoto, *Chemical Oscillations, Waves and Turbulence* (Springer-Verlag, Berlin, 1984); W. van Saarloos, in *Spatiotemporal Patterns in Nonequilibrium Systems*, edited by P.E. Cladis and P. Palffy-Muhoray (Addison-Wesley, Reading, MA, 1994).

[3] For example, see H. Chate, Nonlinearity **7**, 185 (1994) for the $d=1$ CGL equation; H. Chate and P. Manneville, Physica A **224**, 348 (1996) for the $d=2$ CGL equation.

[4] K. Binder, in *Materials Science and Technology, Vol. 5: Phase Transformations of Materials*, edited by R.W. Cahn, P. Haasen, and E.J. Kramer (VCH, Weinheim, 1991), p. 405.

[5] A.J. Bray, Adv. Phys. **43**, 357 (1994).

[6] T. Ohta, D. Jasnow, and K. Kawasaki, Phys. Rev. Lett. **49**, 1223 (1982).

[7] A.J. Bray and S. Puri, Phys. Rev. Lett. **67**, 2670 (1991); H. Toyoki, Phys. Rev. B **45**, 1965 (1992).

[8] G.F. Mazenko Phys. Rev. Lett. **63**, 1605 (1989); Phys. Rev. B **42**, 4487 (1990); **43**, 5747 (1991).

[9] P.S. Hagan, SIAM (Soc. Ind. Appl. Math.) J. Appl. Math. **42**, 762 (1982).

[10] I.S. Aranson, L.B. Aranson, L. Kramer, and A. Weber, Phys. Rev. A **46**, R2992 (1992); A. Weber, L. Kramer, I.S. Aranson, and L.B. Aranson, Physica D **61**, 279 (1992).

[11] A.N. Pargellis, P. Finn, J.W. Goodby P. Panizza, B. Yurke and P.E. Cladis, Phys. Rev. A **46**, 7765 (1992); B. Yurke, A.N. Pargellis, T. Kovacs, and D.A. Huse, Phys. Rev. E **47**, 1525 (1993).

[12] S. Puri, A.J. Bray and F. Rojas, Phys. Rev. E **52**, 4699 (1995); F. Rojas, S. Puri, and A.J. Bray, J. Phys. A **34**, 3985 (2001).

[13] A.J. Bray and K. Humayun, Phys. Rev. E **47**, R9 (1993).

[14] S. K. Das, S. Puri, and M. C. Cross, Phys. Rev. E **64,** 046206 (2001).